15

Non-Catalytic, Low-Temperature Synthesis of Carbon Nanofibers by Plasma-Enhanced Chemical Vapor Deposition

Shinsuke Mori and Masaaki Suzuki
Tokyo Institute of Technology, Japan

1. Introduction

Plasma-enhanced chemical vapour deposition (PECVD) has some unique advantages of allowing low-temperature growth of vertically aligned carbon nanotubes (CNTs) and less crystalline carbon nanofibers (CNFs) (Meyyappan et al., 2003; Melechko et al., 2005). In the conventional PECVD methods for CNTs/CNFs synthesis, metal catalyst particles are used because the CNFs/CNTs are grown by the following steps: (i) adsorption and decomposition of the reactant molecules and their fragments formed in the plasma on a surface of catalyst, (ii) dissolution and diffusion of carbon species through the metal particle, and (iii) precipitation of carbon on the opposite surface of the catalyst particle to form the nanofibers structure (Baker & Harris, 1978; Melechko et al., 2005). Hofmann et al. (2003) have suggested that the rate-determining step for the growth of CNF at a low temperature is not the diffusion of carbon through the catalyst particle bulk, as was proposed by Baker et al. (Baker & Harris, 1978) and is generally accepted for high-temperature conditions, but the diffusion of carbon on the catalyst surface. In this surface diffusion model, carbon atoms adsorbed at the top surface of the metal particles diffuse along the surface, where their motion is much faster than bulk diffusion, and then segregate at the bottom of the particles, forming graphitic planes. These graphitic basal planes are parallel to the metal surface, and the orientation angle between the graphite basal planes and the tube axis is not zero. As a result, although CNFs grown at a higher temperature (> 500 ^{o}C) consist of several graphitic basal planes oriented parallel to the fibre axis with a central hollow region (shell structures; they can be called carbon nanotubes), CNFs grown at a lower temperature consist of stacked cone-segment shaped graphite basal plane sheets (fish-bone, herring-bone, stucked-cone, or stacked-cup structures) or the basal planes oriented perpendicular to the fibre axis (platelets structures) and CNFs with large orientation angles are often not hollow (Fig. 1). For the practical application of CNTs/CNFs, their low-temperature synthesis by PECVD is attractive to achieve the direct deposition of CNTs/CNFs on various substrates involving materials with low melting points. So far, several studies on the low-temperature (< 400^{o}C) synthesis of CNFs/CNTs by PECVD with various discharge systems using hydrocarbons have been reported, such as the RF discharge of CH_4 (Boskovic et al., 2002), the DC discharge of C_2H_2/NH_3 (Hofmann et al., 2003), the AC discharge of $C_2H_2/NH_3/N_2$/He (Kyung et al., 2006), the microwave discharge of CH_4/H_2 (Liao and Ting, 2006), and a

Source: Nanofibers, Book edited by: Ashok Kumar,
ISBN 978-953-7619-86-2, pp. 438, February 2010, INTECH, Croatia, downloaded from SCIYO.COM

combination of ECR C_2H_2 plasma with ICP N_2 plasma (Minea et al., 2004) while few attempts at low-temperature PECVD of CNFs/CNTs using CO as the carbon source have been made (Han et al, 2002; Plonjes et al., 2002).

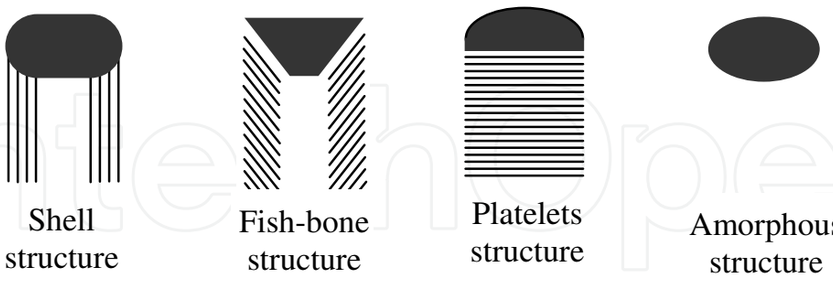

Fig. 1. Schematic cross-sectional illustrations of carbon nanofibers grown by catalytic CVD

The preparation of catalyst particle often limits to lower the process temperature because high-temperature treatment is usually necessary for the activation of catalyst. The elevated temperature is also needed to create the metal particles because metal particles are usually created by breaking up a thin metal film on a substrate into small islands on annealing at elevated temperatures (Merkulov et al., 2000). At the early stage of our CNF synthesis study, the vertically aligned CNFs could be synthesized on a Fe catalyst layer using a $CO/Ar/O_2$ discharge system at extremely low temperatures (Room temperature – 180 ^oC) (Mori et al., 2007, 2008, 2009a). In our subsequent study on the low-temperature activation of metal catalyst particles, it was found that the CNF growth process is not controlled by the catalyst particle, and that, surprisingly, CNFs can be grown even if no catalyst is used in the $CO/Ar/O_2$ plasma system at the optimal growth conditions (Mori & Suzuki, 2009b, 2009c). From the viewpoint of process simplification and product purification, this catalyst-free synthesis is attractive. In this chapter, therefore, we describe only non-catalytic PECVD of CNFs grown at a low-temperature (< 180 ^oC) in a $CO/Ar/O_2$ discharge system.

2. Synthesis

The CNFs were grown using a DC plasma-enhanced CVD system (DC-PECVD) and a microwave plasma-enhanced CVD system (MW-PECVD). In both systems, a low-temperature $CO/Ar/O_2$ plasma was used. In general, the advantages of low-temperature plasma CVD using CO instead of hydrocarbons as the carbon source gas are as follows: (1) the deposition of amorphous carbon is suppressed even at low temperatures (Muranaka et al., 1991; Stiegler et al., 1996); (2) the CO disproportionation reaction, $CO+CO \rightarrow CO_2+C$, is thermodynamically favorable at low temperatures; (3) vibrationally excited molecules are formed which enhance reactions at low temperature, such as $CO(v)+CO(w) \rightarrow CO_2+C$ (Plonjes et al., 2002; Capitelli 1986; Mori et al., 2001); (4) C_2 molecules are known to be formed effectively through the reactions $C + CO + M \rightarrow C_2O + M$ and $C + C_2O \rightarrow C_2 + CO$ and can be precursors for the deposition of functional carbon materials (Caubet & Dorthe, 1994; Ionikh et al., 1994; McCauley et al., 1998).

2.1 DC-PECVD system

Figure 2(a) shows a schematic diagram of the experimental apparatus for the DC-PECVD system. The quartz discharge tube has a 10-mm inner diameter, and there are two electrodes

spaced 5 cm apart and connected to the DC power supply in the discharge tube; one of them is a stainless-steel rod cathode with a diameter of 6 mm and the other is a stainless-steel rod anode with a diameter of 1.5 mm. In this study, borosilicate glass pieces (4 x 4 x 0.2 mm^3) were used as substrates which were placed on the cathode. Before CNF synthesis, the surfaces of substrates were cleaned with ethanol and no catalysts were used in the synthesis. The parameters for the CNFs deposition process were as follows: CO flow rate: 20 sccm, Ar flow rate: 20 sccm; O_2 flow rate: 0-1.0 sccm; total pressure: 800 Pa; discharge current: 2 mA. The substrate temperature, *Ts*, was monitored by a thermocouple placed below the substrate while it would be lower than the upper surface and CNF temperature. Although the substrate was heated up by the discharge, the temperature, *Ts*, of all the samples in this system remained as low as 90 ^oC.

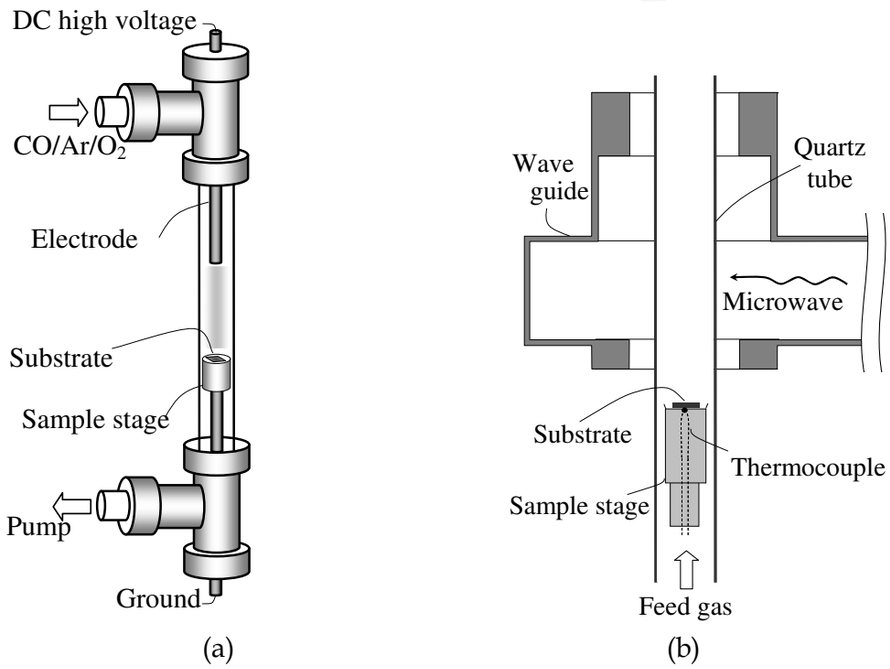

Fig. 2. Schematic diagram of plasma reactor: (a) DC-PECVD and (b) MW-PECVD system

2.2 MW-PECVD system

Figure 2(b) shows a schematic diagram of the MW-PECVD system in which the CNFs were grown. This system comprises a modified ASTeX DPA25 plasma applicator with a quartz discharge tube of 10-mm inner diameter. Borosilicate glass, silicon single-crystal wafers, CaF_2, and polycarbonate plates (4 mm × 4 mm) were used as substrates, and the substrate was placed 52 mm below the center of the waveguide. Before CNF synthesis, the surfaces of substrates were cleaned with ethanol and no catalysts were used in this system. The conditions for CNF deposition process were as follows: CO flow rate, 10 sccm; Ar flow rate, 30 sccm; O_2 flow rate, 0-1.0 sccm; total pressure, 400 Pa; and microwave power, 80 W. The substrate temperature, *Ts*, was monitored by a thermocouple placed below the substrate. In the present configuration, the substrate temperature was automatically increased to about 150 ^oC when plasma irradiation was applied. However, this temperature was unstable. Therefore, in order to achieve steady temperature condition, *Ts* above 150 ^oC was controlled

using a nichrome wire heater equipped with a temperature controllerand maintained stably at 180 ^{o}C throughout the MW-PECVD process.

3. Properties

The carbon deposits growing on the substrate were observed by scanning electron microscopy (Hitachi S-4500, KEYENCE VE-8800) and transmission electron microscopy (JEOL JEM-2010F) and analyzed by Raman spectroscopy (JASCO NRS-2100).

3.1 DC-PECVD system

Figure 3 shows scanning electron microscope (SEM) images of the carbon deposits with different additional O_2 gas compositions. The morphology of carbon deposits is strongly affected by the O_2/CO ratio. Without the addition of oxygen, pillar-like carbon films were formed. When a small amount of O_2 was added to the CO plasma, the morphology of the carbon films changed to a cauliflower-like structure (O_2/CO ~ 1/1000) and a fibrous structure (O_2/CO = 2/1000 ~ 5/1000). At higher O_2 flow rates, however, the deposition rate decreased and the fibrous structure was no longer observed.

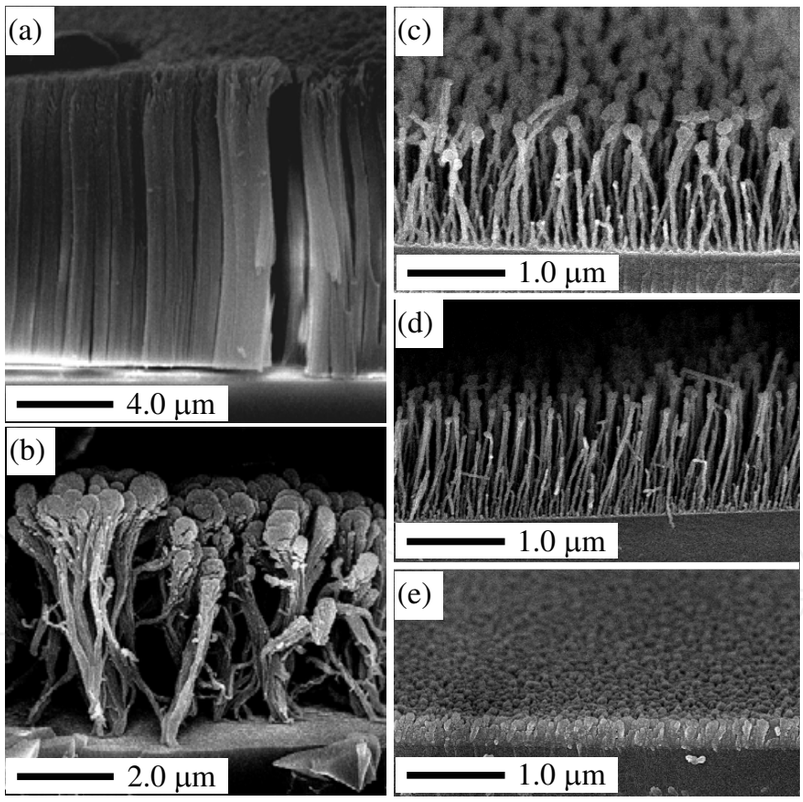

Fig. 3. SEM images of carbon materials synthesized with different O_2/CO ratio without catalyst at 90 ^{o}C. O_2/CO ratio; (a) O_2/CO = 0; (b) O_2/CO = 1/1000; (c) O_2/CO = 2/1000; (d) O_2/CO = 4/1000; (e) O_2/CO = 7/1000: Growth time: (a), (c) 1 h; (b), (d), (e) 2h

Figure 4 shows transmission electron microscope (TEM) images of CNFs synthesized at O_2/CO = 3/1000. Under this condition, the diameter of the CNFs was about 10-50 nm. The

surface of the CNFs was not so smooth. In the high-magnification images, the lattice structure of the crystallized carbon layers is clearly visible. In most of the thinner fibers, the layers were perpendicular to the fiber axis, and it was revealed that the CNFs had a platelet structure [Figs. 4(a) and 4(b)]. That structure has already been reported by some researchers in their catalytic-grown CNFs using carbon monoxide as the carbon source gas (Murayama & Maeda, 1990; Rodriguez et al., 1995; Yoon et al., 2005). In the rest of the fibers, those layers were not clearly seen because their directions were random relative to the fiber axis and they overlapped each other [Figs. 4(d)]. However, it can be said that the crystallinity of the carbon fibers was quite high in spite of the low growth temperature.

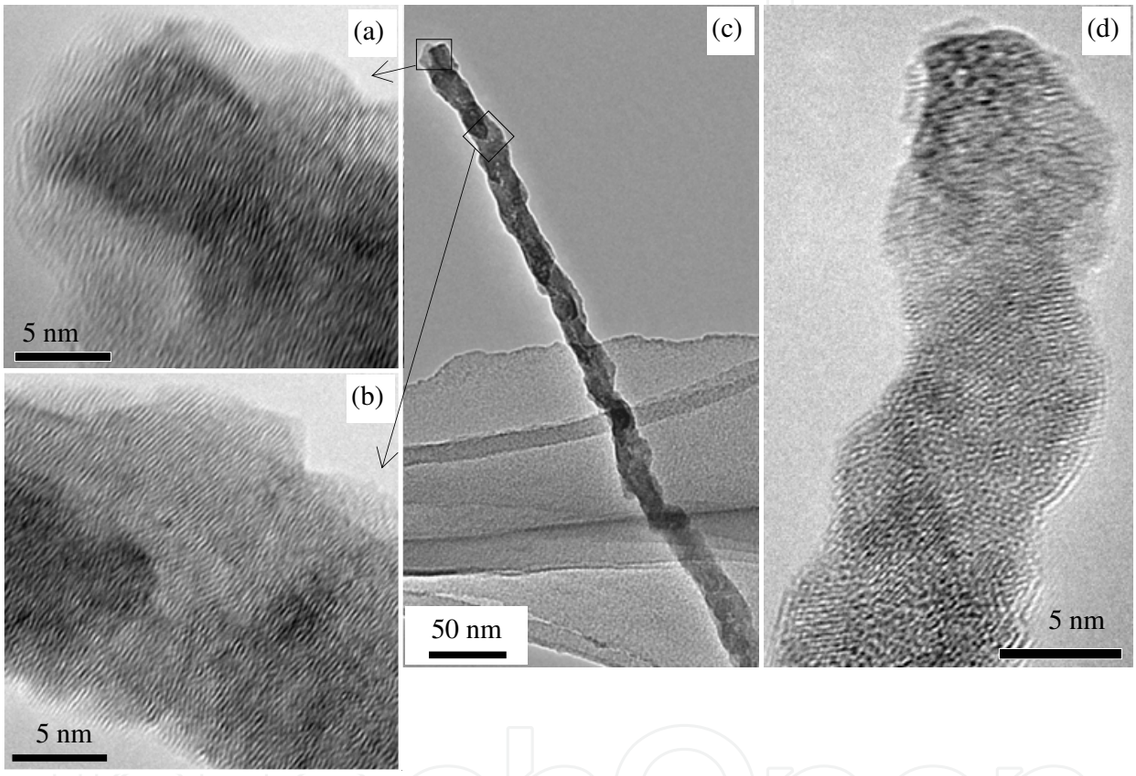

Fig. 4. TEM images of carbon nanofibers synthesized without catalyst at 90 °C. O_2/CO = 3/1000. Growth time: 2 h. (a)-(c) platelets CNFs, (d) randomly oriented CNFs

The Raman spectra of carbon deposits were examined as shown in Fig. 5 and it was found that there was no appreciable difference between the Raman spectra in the present non-catalytic study and previous one in which Fe catalyst was used (Mori & Suzuki, 2008): (1) the spectra for all the samples present two peaks of carbon material: the rather sharp G-band peak at approximately 1590 cm^{-1}, which indicates the presence of crystalline graphene layers, and the broad D-band peak at 1350 cm^{-1}, which indicates the existence of defective graphene layers; (2) the D-band decreased with increasing O_2/CO ratio while the G-band was almost unchanged. Therefore, from the Raman spectroscopic analysis, it is concluded that the deposition of amorphous carbon is selectively suppressed by the addition of O_2.

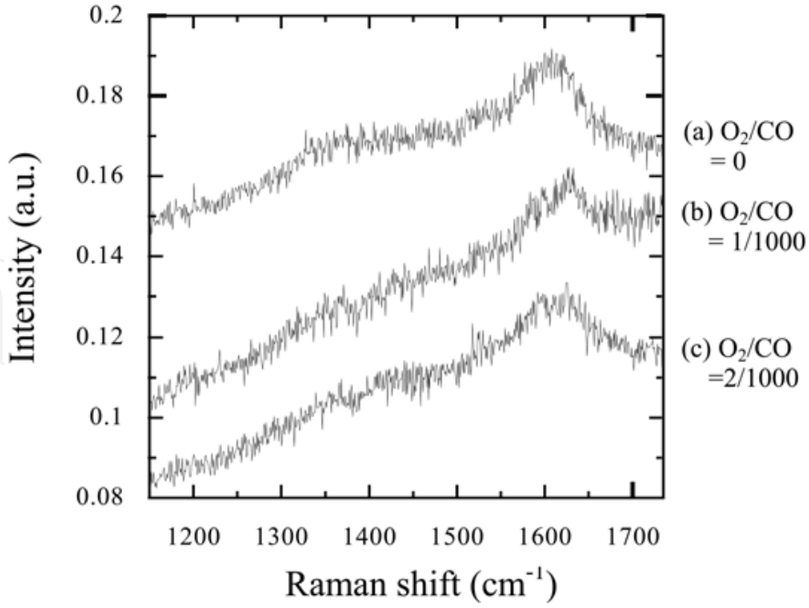

Fig. 5. Raman spectra of the carbon deposits prepared at O_2/CO ratios of; (a) 0/1000; (b) 1/1000; and (c) 2/1000.

3.2 MW-PECVD system

Figure 6 shows SEM images of the carbon deposits grown by MW-PECVD on the glass substrates after 10 minutes of deposition with different levels of O_2 gas supplementation. In the absence of added oxygen, pillar-like carbon films was formed. When a small amount of O_2 was added to the CO plasma, the morphology of the carbon films changed to fibrous structure. At higher O_2 flow rates, however, the deposition rate decreased and no carbon deposits could be observed. While O_2/CO window for CNFs formation is shifted towards a higher O_2 concentration side, the influence of oxygen addition on the morphology of carbon deposits was almost the same as that seen for DC-PECVD system. This is probably due to the fact that in microwave plasma the generation rates of the precursors for carbon deposition, i.e., C and C_2 are much higher than those in DC plasma. Although CNFs synthesized by DC-PECVD are straight, MW-PECVD grown CNFs are slightly waved.

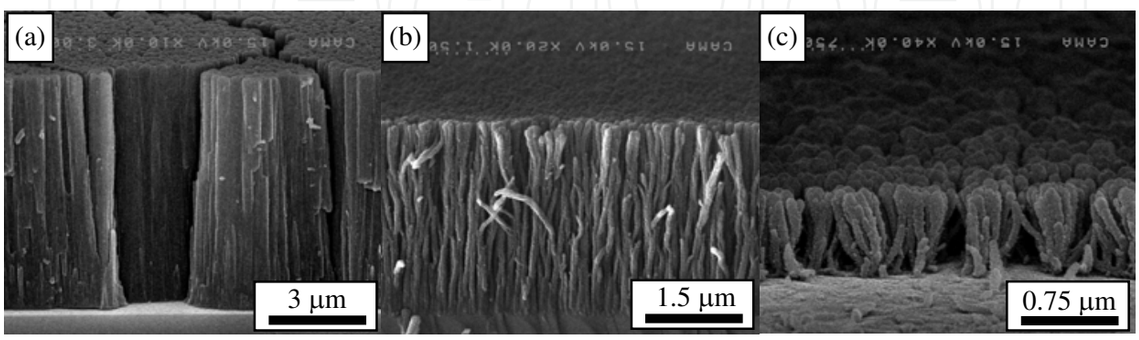

Fig. 6. SEM images of the carbon deposits on the glass substrates at O_2/CO rations of: (a) 0/1000; (b) 7/1000; and (c) 9/1000

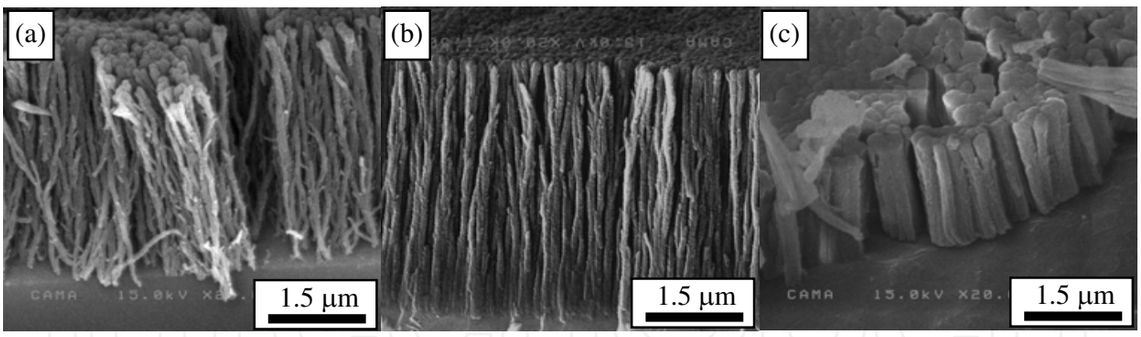

Fig. 7. SEM images of carbon deposits on different substrate materials.
Substrates: (a) CaF_2; (b) Si; (c) polycarbonate

Figure 7 shows SEM images of CNFs grown on different material substrates. The morphologies of the CNFs grown on Si and CaF_2 substrates were almost the same as those grown on the glass substrates. However, CNFs grown on the polycarbonate showed a different morphology. The diameters of the CNFs were increased, fiber-bundling was evident, and the fiber length was diminished. The high affinity that exists between the precursor species and organic materials may result in the formation of large nuclei on the substrates and result in the growth of CNFs with large diameter.

Figure 8 shows TEM images of the CNFs. The diameters of CNFs were 50-100 nm and no tubular structure was evident (Fig.8(a)). The surfaces of the CNFs were covered with the branching fibers and their nuclei, whose diameters are 5-10 nm. The high-magnification image of the CNF edge is shown in Fig. 8(b). Although it is not clearly seen because they overlapped and their directions were random in relation to the fiber axis, the lattice images of crystallized carbon were partially observed especially in the branching fibers.

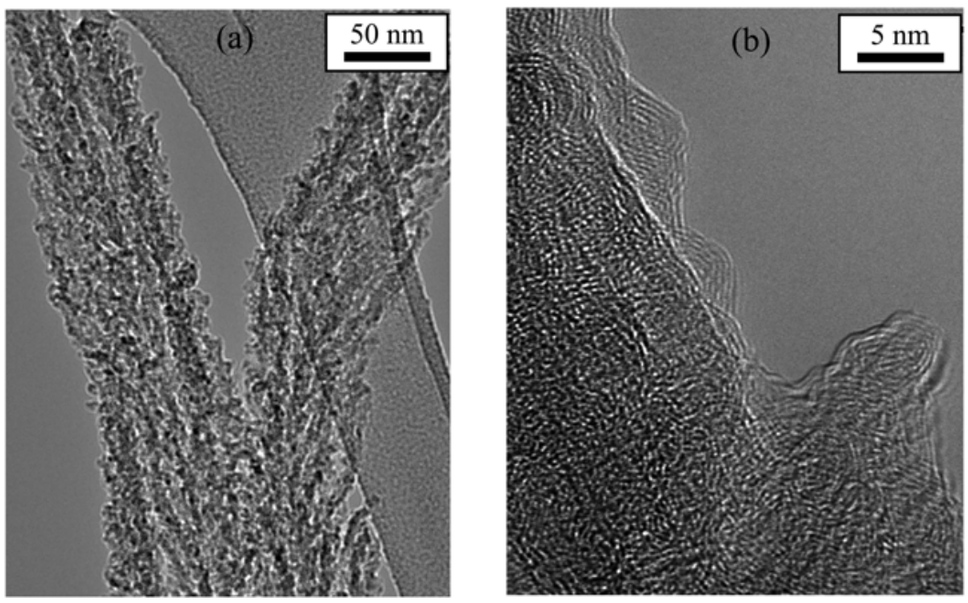

Fig. 8. TEM images of CNFs grown on the glass substrates at an O_2/CO ratio of 7/1000. (a) Low-magnification TEM image of two bundling CNFs; (b) high-magnification TEM image of the CNF surface.

The Raman spectra for the carbon materials formed on the glass substrate by MW-PECVD system were also examined. As shown in Figure 9, the rather sharp G-band peak and the broad D-band peak were observed and the D-band peak at 1350 cm^{-1}decreased with increasing O_2 flow rate, which is similar to the DC-PECVD results.

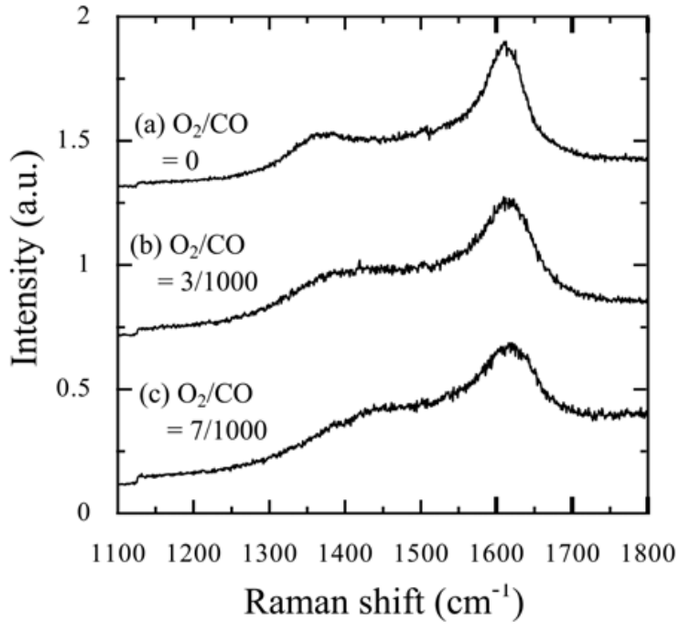

Fig. 9. Raman spectra of the carbon deposits prepared at O_2/CO ratios of; (a) 0/1000; (b) 3/1000; and (c) 7/1000.

4. Reaction mechanism and growth model

In order to infer the reaction mechanism, the plasma emission was monitored by a spectrometer (Ocean Optics, HR4000). The typical emission spectra from CO/Ar/O_2 plasma were shown in Fig. 10. A strong C_2 high-pressure band and CO Angstrom bands ($B^1\Sigma+ \rightarrow A^1\Pi$) and also a weak C atom spectrum at 247.9 nm can be seen. Interestingly, instead of C_2 swan bands ($d^3\Pi_g \rightarrow a^3\Pi_u$), which are well known as the most prominent bands of C_2 in hydrocarbon discharge and combustion flames, C_2 high-pressure bands ($d^3\Pi_g$, v=6 $\rightarrow$ $a^3\Pi_u$) were observed in this system, which are known to be predominant compared to other C_2 band systems under certain CO discharge conditions (Caubet et al., 1994).

Figure 11 shows the influence of oxygen fraction on the emission intensities of CO Angstrom band, C_2 HP band, and C atom spectra. From this figure, the contribution of C_2 molecules to the CNF synthesis is suggested, because it is only C_2 molecules that the emission intensity shows a substantial change when the amount of oxygen increases. As for atomic carbon, the emission intensity is not influenced by the addition of oxygen and it is thought that there is no substantial change in the amount of C atom concentration.

It is more clearly suggested from Fig. 12 in which the normalized growth rate of CNFs and emission intensity of CO, C and C_2 by those without oxygen addition are plotted as a function of oxygen fraction. Although the normalized emission intensity of C atom spectra are not influenced by the addition of oxygen, that of C_2 HP band and normalized growth

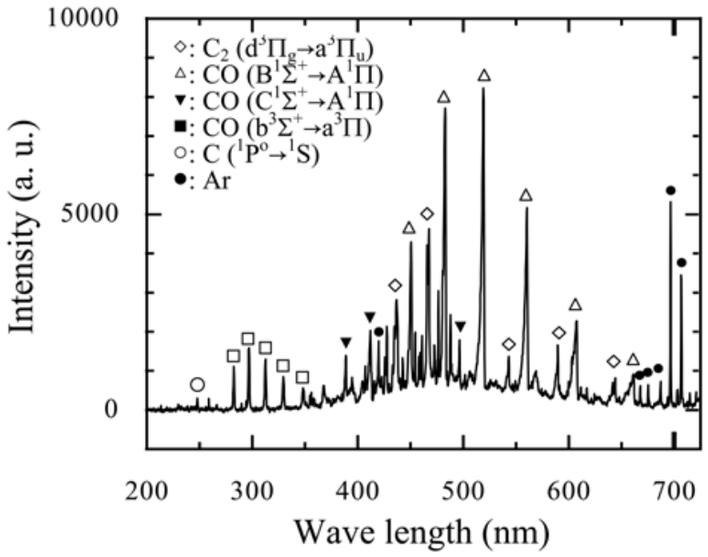

Fig. 10. Typical Emission Spectra of CO/Ar Plasma from the cathode region (O_2/CO = 0)

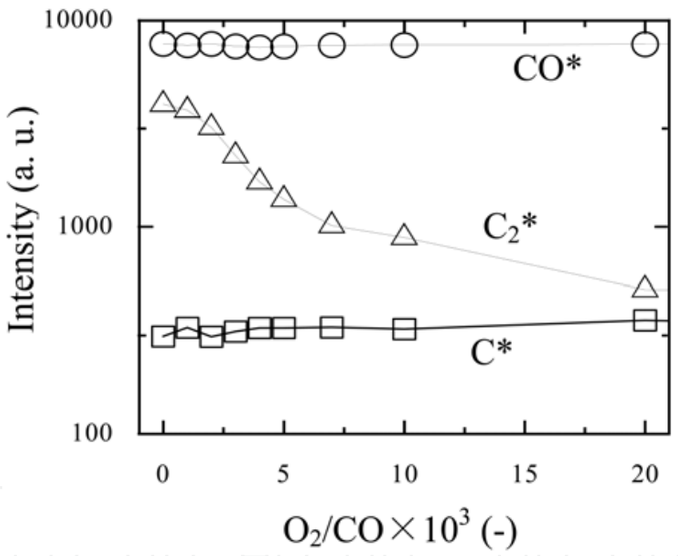

Fig. 11. Emission intensity of CO*, C_2*, and C* as a function of O_2/CO ratio

rates decrease drastically with increasing additional oxygen fraction and show a good correlation between them. In general, the change in the precursor density and the increase in the etching ability are thought to be the reasons why CNFs disappears as the amount of oxygen increases. However, as shown in the previous study, it cannot be thought that an increase in the etching ability is the reason for the disappearance of the CNFs in this case. When the small amount of hydrogen was added to the CO/Ar plasma, the CNFs disappear but the carbon deposits are not removed. As for the change in the spectrum, it is only C_2 molecules that the emission intensity shows a substantial change when the amount of hydrogen increases (Mori & Suzuki, 2008). In other words, even if the etching ability is low, the suppression of C_2 molecule formation results in the disappearance of fibrous structure. The carbon etching ability of hydrogen is much lower than that of oxygen (Mucha et al.,

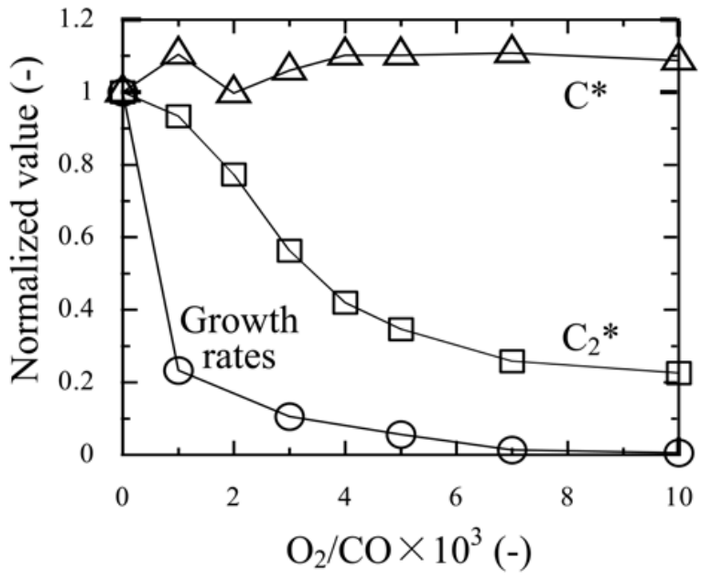

Fig. 12. Normalized growth rates of CNFs and emission intensities of C_2* and C* as a function of O_2/CO ratio. In this figure, growth rates and emission intensities are normalized using their values at O_2/CO = 0

1989). Therefore, it is reasonable to assume that, instead of C atoms, C_2 molecules play an important role as the main precursors of CNF synthesis in this system.

Although the growth mechanism for the formation of fibrous structure without catalyst metal particles has not been clearly understood yet, the nucleation and island growth process can be a key to control the morphology of carbon materials and the dispersed nuclei play the role of growth site for the CNFs. This is because CNFs grown on the polycarbonate has different morphology as shown in Fig. 7. The diameter of CNF grown on the polycarbonate is increased and fiber bundling arises and the length of fiber is diminished. The large affinity between precursor species and organic materials would result in the formation of large nuclei on the substrates and result in the growth of CNFs with large diameter (Mori & Suzuki, 2009c). In addition, the termination of the CNF surface by the oxygen would also be the key for the linear growth because the FTIR spectra of CNF includes a lot of oxygen containing groups, which is similar to C_3O_2 polymers and C_3O_2 polymers was known to have a linear structure (Mori & Suzuki, 2009a; Blake et al., 1964). It would be also ascribed to the anisotropic crystallization at the tip of the fiber due to the anisotropic action normal to the substrates in the cathode sheath region such as ion bombardment. Furthermore, C_2 molecules, which are known to be formed effectively in CO plasma, may crystallize anisotropically more readily than C atoms, thereby enhancing the linear growth of the CNFs.

Based on the results described above, the following model was postulated for the non-catalytic CNF growth mechanism. At first, precursor species such as C and C_2 appear mainly in the negative glow area, in which strong emission from C_2 molecules are observed, and diffuse to the substrate. Then, the Volmer–Weber island growth occurs on the substrate. During this nucleation process, if the affinity between the substrate and precursor species is high, then the diameters of the nuclei become large and the fibrous structure disappears.

Next, the carbon film grows up from the nucleus. During this nucleation and growth process, the precursor species deposited on the substrate are etched by the oxygen selectively, and only the crystallized carbons on the nuclei remain (Muranaka et al., 1991; Stiegler et al., 1996). Because of the etching action of oxygen on the nuclei, amorphous carbon, which tends to grow isotropically, is selectively removed, and only the crystallized carbon (graphitic carbon) remains anisotropically (Muranaka et al., 1991; Stiegler et al, 1996; Mucha et al., 1989). Moreover, because of the surface diffusion of the etchant species from the substrate and/or that of the precursor species to the substrate, the growth rate on the nucleus near the substrate is slower than at the tip area, which results in anisotropic growth from the nuclei. After some growth of the nuclei, the local deposition of precursor species occurs around the tip area, which leads the anisotropic growth. This is because the sticking probability of the precursor species onto the CNF surface is so high (Traskelin et al., 2008) that almost all of the precursor species are deposited around the tip area and rarely reach the lower fiber surface. In this anisotropic growth process, if the O_2/CO ratio is optimal, the diameter of CNFs does not increase as the fiber grows, and a fibrous structure can be achieved. However, if the O_2/CO ratio is slightly lower than its optimum value, the diameter of the CNFs increases as the fiber grows and the CNFs attach to adjacent fibers, which finally extinguishes the fibrous structure. On the other hand, if the O_2/CO ratio is slightly higher than its optimum value, the diameter of CNFs decreases as the fiber grows or nuclei can not grow further. The additional oxygen leads not only to amorphous carbon etching but also to the suppression of C_2 molecules formation by scavenging C_2O radicals (Mori & Suzuki, 2009d), which results in the disappearance of the fibrous structure and suppression of the carbon deposition. This optimum O_2/CO window is so narrow that this phenomenon would not have been observed until now.

5. Conclusion

The morphology of carbon deposits in the CO/Ar/O_2 plasma system is strongly affected by the O_2/CO ratio and, at the optimal O_2/CO ratio, vertically aligned CNFs were synthesized at a extremely low temperature in the absence of catalyst. The optimum O_2/CO ratio is crucial for the synthesis of CNFs without catalyst, as it suppresses the isotropic deposition of carbon materials by etching the amorphous carbon selectively and facilitates the anisotropic linear growth of carbon deposits by allowing the formation of crystallized carbon. The spectroscopic study reveals that there is a strong correlation between C_2 formation and CNF growth and C_2 molecules play an important role as the main precursors of CNF synthesis in the CO/Ar/O_2 PECVD system. The nucleation and island growth process is a key to control the morphology of carbon materials and the dispersed nuclei play the role of growth site for the CNFs. In addition, the termination of the CNF surface by the oxygen would also be an important factor for the linear growth of carbon materials without catalyst. From the viewpoint of process simplification and product purification, this catalyst-free synthesis is attractive. As is well known, high-temperature treatment is usually necessary for the activation of catalyst in the conventional CNFs growth method; the non-catalytic synthesis could lead to the development of a more viable process for the direct growth of CNFs onto low-temperature substrates like plastics, because no catalyst preparation step would be necessary.

6. Acknowledgments

We thank Mr. Katsuaki Hori, Mr. Akira Genseki, and Mr. Jun Koki of the Center for Advanced Material Analysis in Tokyo Institute of Technology for assistance with the SEM and TEM observations.

7. References

Baker, R.T.K. & P.S. Harris (1978). The formation of filamentous carbon, *Chemistry and Physics of Carbon*, Vol. 14, p. 83, Marcel Dekker, New York

Blake, A.R., W.T. Eeles & P.P. Jennings (1964). Carbon suboxide polymers, *Trans. Faraday Soc.*, Vol. 60, pp. 691-699

Boskovic, B.O., V. Stolojan, R.U.A. Khan, S. Haq & S.R.P. Silva (2002). Large-area synthesis of carbon nanofibres at room temperature, *Nat. Mater.*, Vol. 1, pp. 165-168

Capitelli, M. (1986). *Nonequilibrium Vibrational Kinetics*, Springer, ISBN 3-540-16250-X, Berlin

Caubet, P. & G. Dorthe (1994). Origin of C_2 high-pressure bands observed in the products of a microwave discharge through CO, *Chem. Phys. Lett.*, Vol. 218, pp. 529-536

Han, J.H., S.H. Choi, T.Y. Lee, J.B. Yoo, C.Y. Park, T.W. Jeong, H.J. Kim, Y.J. Park, I.T. Han, J.N. Heo, C.S. Lee, J.H. Lee & W.K. Yi (2002). Field emission properties of modified carbon nanotubes grown on Fe-coated glass using PECVD with carbon monoxide, *Physica B Condens. Matter*, Vol. 323, pp. 182-183

Hofmann, S., C. Ducati, J. Robertson & B. Kleinsorge (2003). Low-temperature growth of carbon nanotubes by plasma-enhanced chemical vapor deposition, *Appl. Phys. Lett.*, Vol. 83, pp. 135-137

Ionikh, Yu Z., I.N. Kostyukevich & N.V. Chernysheva (1994). Excitation of swan bands of a C_2 molecule in steady-state and decaying plasma in a He-CO mixture, *Opt. Spectrosc.*, Vol. 76, pp. 361-367

Kyung, S.-J., Y.-H. Lee, C.-W. Kim, J.-H. Lee & G.-Y. Yeom (2006). Field emission properties of carbon nanotubes synthesized by capillary type atmospheric pressure plasma enhanced chemical vapor deposition at low temperature, *Carbon*, Vol. 44, pp. 1530-1534

Liao, K.-H. & J.-M. Ting (2006). Characteristics of aligned carbon nanotubes synthesized using a high-rate low-temperature process, *Diamond Relat. Mater.*, Vol. 15, pp. 1210-1216

McCauley, T.G., D.M. Gruen & A.R. Krauss (1998). Temperature dependence of the growth rate for nanocrystalline diamond films deposited from an Ar/CH_4 microwave plasma, *Appl. Phys. Lett.*, Vol. 73, pp. 1646-1648

Melochko A.V., V.I. Merkulov, T.E. McKnight, M.A. Guillorn, K.L. Klein, D.H. Lowndes & M.L. Simpson (2005). Vertically aligned carbon nanofibers and related structures; Controlled synthesis and directed assembly, *J. Appl. Phys.*, Vol. 97, pp. 041301-1-39

Merkulov, V.I., D.H. Lowndes, Y.Y. Wei, G. Eres & E. Voelkl (2000). Patterned growth of individual and multiple vertically aligned carbon nanofibers, *Appl. Pys. Lett.*, Vol. 76, pp. 3555-3557

Meyyappan, M, L. Delzeit, A. Cassell & D. Hash (2003). Carbon nanotubes growth by PECVD; a review, *Plasma Source Science Technol.*, Vol. 12, pp. 205-216

Minea, T.M, S. Point, A. Granier & M. Touzeau (2004). Room temperature synthesis of carbon nanofibers containing nitrogen by plasma-enhanced chemical vapor deposition, *Appl. Phys. Lett.*, Vol. 85, pp. 1244-1246

Mori, S., H. Akatsuka & M. Suzuki (2001). Carbon and oxygen isotope separation by plasma chemical reactions in carbon monoxide glow discharge, *J. Nucl. Sci. Technol.*, Vol. 38, pp. 850-858

Mori, S., M. Fukuya & M. Suzuki (2007). Synthesis of carbon nanofibers using carbon monoxide DC plasma at room temperature, *Trans. Mater. Res. Soc. Jpn.*, Vol. 32, pp. 513-516

Mori, S. & M. Suzuki (2008). Effect of oxygen and hydrogen addition on the low-temperature synthesis of carbon nanofibers using a low-temperature CO/Ar DC plasma, *Diamond Relat. Mater.*, Vol. 17, pp. 999-1002

Mori, S. & M. Suzuki (2009a). Characterization of carbon nanofibers synthesized by microwave plasma-enhanced CVD at low-temperature in a $CO/Ar/O_2$ system, *Diamond Relat. Mater.*, Vol. 18, pp. 678-681

Mori, S. & M. Suzuki (2009b). Non-catalytic low-temperature synthesis of carbon nanofibers by plasma-enhanced chemical vapour deposition in a $CO/Ar/O_2$ DC discharge system, *Appl. Phys. Exp.*, Vol. 2, pp. 015003-1-3

Mori, S. & M. Suzuki (2009c). Catalyst-free low-temperature growth of carbon nanofibers by microwave plasma-enhanced CVD, *Thin Solid Films*, Vol. 517, pp. 4264-4267

Mori, S. & M. Suzuki (2009d). The role of C_2 in low temperature growth of carbon nanofibers, *J. Chem. Eng. Jpn.*, in press

Mucha, J.A., D.L. Flamm & D.E. Ibbotson (1989). On the role of oxygen and hydrogen in diamond-forming discharges, *J. Appl. Phys.*, Vol. 65, pp. 3448-3452

Muranaka, Y., H. Yamashita, H. Miyadera (1991). Characterization of diamond films synthesized in the microwave plasmas of CO/H_2 and $CO/O_2/H_2$ systems at low temperatures (403-1023 K), *J. Appl. Phys.*, Vol. 69, pp. 8145-8152

Murayama, H & T. Maeda (1990). A novel form of filamentous graphite, *Nature*, Vol. 345, pp. 791-793

Plonjes, E., P. Palm, G.B. Viswanathan, V.V. Subramaniam, I.V. Adamovich, W.R.Lempert, H.L. Fraser & J.W. Rich (2002). Synthesis of single-walled carbon nanotubes in vibrationally non-equilibrium carbon monoxide, *Chem. Phys. Lett.*, Vol. 352, pp. 342-347

Rodriguez, N.M. A. Chambers & R.T.K. Baker (1995). Catalytic engineering of carbon nanostructures, *Langmuir*, Vol. 11, pp. 3862-3866

Stiegler, J., T. Lang, M. Nygard-Ferguson, Y.von Kaenel & E. Blank (1996). Low temperature limits of diamond film growth by microwave plasma-assisted CVD, *Diamond Relat. Mater.*, Vol. 5, pp. 226-230

Traskelin, P., O. Saresoja & K. Nordlund (2008). Molecular dynamics simulations of C_2, C_2H, C_2H_2, C_2H_3, C_2H_4, C_2H_5, and C_2H_6 bombardment of diamond (1 1 1) surfaces, *J. Nucl. Mater.*, Vol. 375, pp. 270-274

Yoon, S.-H., S. Lim, S.-h. Hong, W. Qiao, D.D. Whitehurst, I. Mochida, B. An & K. Yokogawa (2005). A conceptual model for the structure of catalytically grown carbon nanofibers, *Carbon*, Vol. 43, pp. 1828-1838

Nanofibers

Edited by Ashok Kumar

ISBN 978-953-7619-86-2
Hard cover, 438 pages
Publisher InTech
Published online 01, February, 2010
Published in print edition February, 2010

“There’s Plenty of Room at the Bottom” this was the title of the lecture Prof. Richard Feynman delivered at California Institute of Technology on December 29, 1959 at the American Physical Society meeting. He considered the possibility to manipulate matter on an atomic scale. Indeed, the design and controllable synthesis of nanomaterials have attracted much attention because of their distinctive geometries and novel physical and chemical properties. For the last two decades nano-scaled materials in the form of nanofibers, nanoparticles, nanotubes, nanoclays, nanorods, nanodisks, nanoribbons, nanowhiskers etc. have been investigated with increased interest due to their enormous advantages, such as large surface area and active surface sites. Among all nanostructures, nanofibers have attracted tremendous interest in nanotechnology and biomedical engineering owing to the ease of controllable production processes, low pore size and superior mechanical properties for a range of applications in diverse areas such as catalysis, sensors, medicine, pharmacy, drug delivery, tissue engineering, filtration, textile, adhesive, aerospace, capacitors, transistors, battery separators, energy storage, fuel cells, information technology, photonic structures and flat panel displays, just to mention a few. Nanofibers are continuous filaments of generally less than about 1000 nm diameters. Nanofibers of a variety of cellulose and non-cellulose based materials can be produced by a variety of techniques such as phase separation, self assembly, drawing, melt fibrillation, template synthesis, electro-spinning, and solution spinning. They reduce the handling problems mostly associated with the nanoparticles. Nanoparticles can agglomerate and form clusters, whereas nanofibers form a mesh that stays intact even after regeneration. The present book is a result of contributions of experts from international scientific community working in different areas and types of nanofibers. The book thoroughly covers latest topics on different varieties of nanofibers. It provides an up-to-date insightful coverage to the synthesis, characterization, functional properties and potential device applications of nanofibers in specialized areas. We hope that this book will prove to be timely and thought provoking and will serve as a valuable reference for researchers working in different areas of nanofibers. Special thanks goes to the authors for their valuable contributions.

How to reference

In order to correctly reference this scholarly work, feel free to copy and paste the following:

Shinsuke Mori and Masaaki Suzuki (2010). Non-Catalytic, Low-Temperature Synthesis of Carbon Nanofibers by Plasma-Enhanced Chemical Vapor Deposition, Nanofibers, Ashok Kumar (Ed.), ISBN: 978-953-7619-86-2, InTech, Available from: http://www.intechopen.com/books/nanofibers/non-catalytic-low-temperature-synthesis-of-carbon-nanofibers-by-plasma-enhanced-chemical-vapor-depos

INTECH
open science | open minds

InTech Europe
University Campus STeP Ri
Slavka Krautzeka 83/A
51000 Rijeka, Croatia
Phone: +385 (51) 770 447
Fax: +385 (51) 686 166
www.intechopen.com

InTech China
Unit 405, Office Block, Hotel Equatorial Shanghai
No.65, Yan An Road (West), Shanghai, 200040, China
中国上海市延安西路65号上海国际贵都大饭店办公楼405单元
Phone: +86-21-62489820
Fax: +86-21-62489821

IntechOpen